

Addition Spectra of Quantum Dots in Strong Magnetic Fields

S.-R. Eric Yang,^{1,2} A. H. MacDonald,² and M. D. Johnson³

¹*Institute for Materials Research, National Research Council of Canada, Ottawa, Canada K1A 0R6*

²*Department of Physics, Indiana University, Bloomington, Indiana 47405*

³*Department of Physics, University of Central Florida, Orlando, Florida 32816-2385*

(Received 3 June 1993)

We consider the magnetic field dependence of the chemical potential for parabolically confined quantum dots in a strong magnetic field. Approximate expressions based on the notion that the size of a dot is determined by a competition between confinement and interaction energies are shown to be consistent with exact diagonalization studies for small quantum dots. Fine structure is present in the magnetic field dependence which cannot be explained without a full many-body description and is associated with ground-state level crossings as a function of confinement strength or Zeeman interaction strength. Some of this fine structure is associated with precursors of the bulk incompressible states responsible for the fractional quantum Hall effect.

PACS numbers: 73.20.Dx, 73.20.Mf

Advances in nanofabrication technology have made it possible to manufacture "quantum dots" in which electrons are confined to a small area within a two-dimensional (2D) electron gas [1]. Interest in these systems has grown as a result of recently developed techniques [2,3] which probe them spectroscopically. The quantity which is measured [4] in these experiments is the magnetic field dependence of the "addition spectrum," i.e., the energy to add one electron to a dot. This is given by $\mu_N \equiv E_N^0 - E_{N-1}^0$, where E_N^0 is the ground state energy of an N -electron dot. Addition spectrum measurements have generally been interpreted in terms of "constant interaction" models in which electron-electron interactions are accounted for by including a charging energy which is characterized by a fixed self-capacitance; or, when this fails, by using Hartree or Hartree-Fock approximations. However, especially at strong magnetic fields, quantum dots can have strongly correlated [5,6] ground states, some of which are precursors of the bulk incompressible states responsible for the fractional quantum Hall effect. In this regime a complete interpretation of addition spectra measurements requires an exact treatment of the Coulombic electron-electron interactions.

In this Letter we report on numerical exact diagonalization calculations of the addition spectrum for quantum dots in a strong magnetic field. We find that the addition spectrum has a surprisingly rich magnetic field dependence, showing a large number of sharp features superimposed on a smooth background. The background can be accounted for using a simple Hartree approximation. The sharp features are associated with energy-level crossings at fixed N , often between strongly correlated states. The spin degree of freedom has a nontrivial role, in general not consistent with expectations based on the Hartree-Fock approximation. The constant interaction model fails qualitatively for strong magnetic fields.

We consider a system of 2D electrons confined by a parabolic potential [7], $V(r) = m\Omega^2 r^2/2$. We confine our attention here to the strong magnetic field limit [8],

$\Omega/\omega_c \leq 1$. ($\omega_c \equiv eB_\perp/m^*c$, where B_\perp is the component of the magnetic field perpendicular to the 2D layer.) In this limit [1] the symmetric gauge single-particle eigenstates are conveniently classified by a Landau level index n and an angular momentum index $m \geq -n$, and we can confine our attention to $n = 0$. The single-particle orbitals in the $n = 0$ level have energies $\varepsilon_m = \hbar\omega_c/2 + \gamma(m+1)$, where $\gamma = m^*\Omega^2\ell^2$ and $\ell^2 \equiv \hbar c/eB_\perp$. [$\langle m|r^2|m \rangle = 2\ell^2(m+1)$.] Hereafter we absorb the constant $\hbar\omega_c/2$ into the zero of energy, and use as the unit of energy the interaction energy $e^2/\epsilon\ell$. The many-electron energies are then determined by two dimensionless numbers characterizing the ratio of the confinement and Zeeman energies to the interaction energy; $\tilde{\gamma} \equiv \gamma/(e^2/\epsilon\ell)$ and $\tilde{g} \equiv g\mu B/(e^2/\epsilon\ell)$. Note that we explicitly include the possibility of tilted fields since we believe that tilted-field experiments will prove to be very valuable.

The Hamiltonian is invariant under spatial rotations about an axis perpendicular to the 2D plane and passing through the center of the dot, and also under rotations in spin space about the magnetic field direction ($\hat{\alpha}$). It follows that both the total angular momentum M_z and $S_\alpha \equiv \mathbf{S} \cdot \hat{\alpha}$ are good quantum numbers. Eigenenergies may be expressed as a sum of interaction and single-particle contributions,

$$E_i(N, M_z, S_\alpha) = U_i(N, M_z, S_\alpha) + \gamma(N + M_z) - g\mu_B B S_\alpha. \quad (1)$$

Here i labels a state within a (M_z, S_α) subspace, and $U_i(N, M_z, S_\alpha) \propto e^2/\epsilon\ell$ is determined by exactly diagonalizing the electron-electron interaction term in the Hamiltonian within this subspace [9]. We have used a Lanczos algorithm to determine the minimum interaction energy within each subspace, $U_0(N, M_z, S_\alpha)$. For $N = 2, 3, 4, 5, 6$ we have considered all possible values of S_α , while for $N = 7, 8$ we have considered only fully spin polarized states with $S_\alpha = N/2$. In each case we have considered all values of M_z from the minimum value con-

sistent with the Pauli exclusion principle (see below) to $M_z = 3N(N - 1)/2$, which is large enough to accommodate an $m = 3$ Laughlin droplet [10,11]. For given values of $\tilde{\gamma}$ and \tilde{g} the ground state subspace is determined by minimizing $E_0(N, M_z, S_\alpha)$ with respect to M_z and S_α . This procedure results in a surprisingly rich phase diagram.

Results for $N = 5$ and $N = 6$ are shown in Figs. 1 and 2. Regions in the phase diagram are labeled by the quantum numbers of the state with lowest energy. Along the boundary lines in these phase diagrams ground state level crossings occur; the slope of a line is given by $(S_\alpha - S'_\alpha)/(M_z - M'_z)$ and the intercept by $[U_0(N, M'_z, S'_\alpha) - U_0(N, M_z, S_\alpha)]/(M_z - M'_z)$. In each spin multiplet the only ground state candidate for any nonzero \tilde{g} is the state which is polarized along the field, i.e., $S_\alpha = S$. Thus the S_α values in these figures give the total spin quantum numbers of the corresponding states.

We discuss these rather complicated phase diagrams, beginning with \tilde{g} and $\tilde{\gamma}$ relatively large, on the upper right-hand side of the lower panels. For $N = 5$ only the (4,1), (6,3), and (10,5) re-

gions in the phase diagram correspond to the single-Slater-determinant ground states which would be obtained in the Hartree-Fock approximation. The occupation numbers for these states are given by $(\bullet\bullet\bullet\circ; \bullet\bullet\circ)$, $(\bullet\bullet\bullet\bullet\circ; \bullet\circ)$, and $(\bullet\bullet\bullet\bullet\bullet\circ; \circ)$, respectively. [An occupied (unoccupied) single-particle state is represented by a full (empty) circle. Circles left (right) of the semicolon represent spin up (down) states. The angular momentum m of a single-particle state increases from left to right.] Similarly, for $N = 6$ the (6,0), (7,2), (10,4), and (15,6) regions have single-Slater-determinant ground states with occupation numbers given by $(\bullet\bullet\bullet\circ; \bullet\bullet\bullet\circ)$, $(\bullet\bullet\bullet\bullet\circ; \bullet\bullet\circ)$, $(\bullet\bullet\bullet\bullet\bullet\circ; \bullet\circ)$, and $(\bullet\bullet\bullet\bullet\bullet\bullet\circ; \circ)$, respectively. The (4,1) state for $N = 5$ and the (6,0) state for $N = 6$ minimize the confinement energy and are ground states at all values of $\tilde{\gamma}$ in the absence of other interactions. These states are the precursors of the Landau level filling factor $\nu = 2$ states for bulk systems.

As the confinement strength $\tilde{\gamma}$ weakens, interactions favor less compact (larger M_z) electron dots. [$U_0(N, M_z + 1, S_\alpha) \leq U_0(N, M, S_\alpha)$.] For these dot sizes the expansion first occurs, except at small \tilde{g} , by forming the most compact states consistent with increasing spin polarization until complete polarization is reached. For large \tilde{g} , states with large spin quantum numbers are favored; eventually, for very large \tilde{g} , only states with $S = N/2$ occur. The tendency toward complete spin polarization

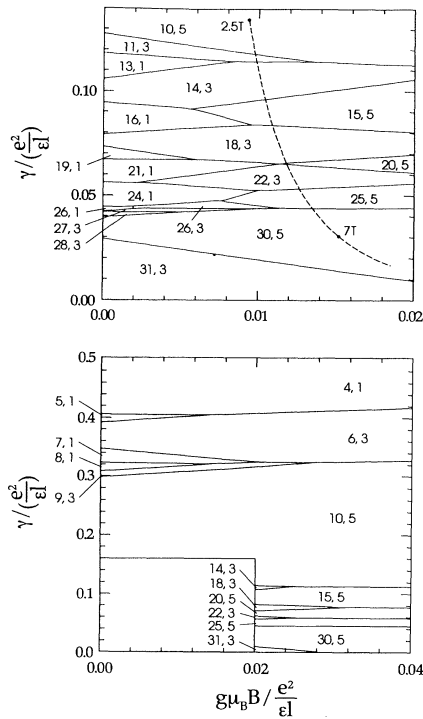


FIG. 1. Phase diagram for a $N = 5$ parabolically confined quantum dot. Regions in the phase diagram are labeled by the M_z and $N_\uparrow - N_\downarrow$ values of the ground state. [$S_\alpha = (N_\uparrow - N_\downarrow)/2$.] The upper panel shows the rich behavior at weak confinement which is related to the physics of the fractional quantum Hall effect. The dashed line shows the path in the phase diagram followed by GaAs sample with $\hbar\Omega = 2$ meV and a perpendicular magnetic field between $B = 2.5$ T and $B = 7$ T.

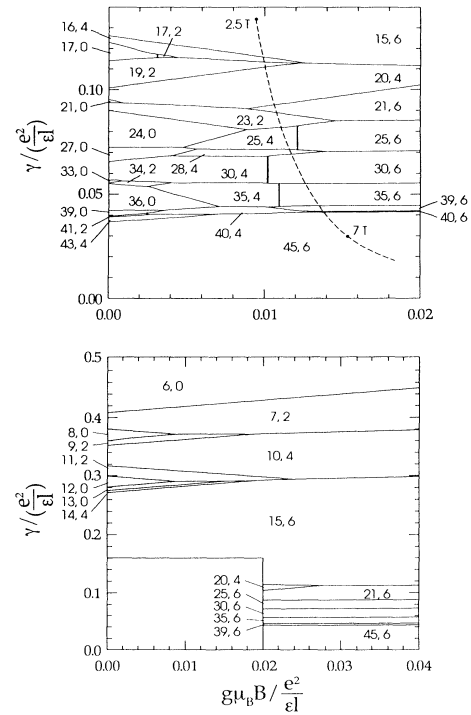


FIG. 2. Phase diagram for a $N = 6$ parabolically confined quantum dot. Regions in the phase diagram are labeled as in Fig. 1.

is what simplifies the phase diagram at larger values of \tilde{g} . At small \tilde{g} , as the confinement $\tilde{\gamma}$ weakens the dot expands by introducing holes [11,12] into the dot. As these holes begin to correlate the Hartree-Fock approximation begins to fail. One consequence is that interactions often favor states which are not completely spin polarized. At weaker confinement the ground states are linear combinations of many Slater determinants. Many of the states which occur can be identified as precursors of the bulk incompressible states responsible for the fractional quantum Hall effect. For example, for $N = 5$ the (30,5) region corresponds to the $\nu = \frac{1}{3}$ state while for $N = 6$ the (36,0) and (45,6) phase regions correspond to the $\nu = \frac{2}{5}$ spin-singlet state and $\nu = \frac{1}{3}$ spin-polarized states.

States with larger values of M_z occur and the phase diagram becomes richer as $\tilde{\gamma}$ decreases. The upper panels in Figs. 1 and 2 show the small \tilde{g} , small $\tilde{\gamma}$ regions of the phase diagrams on an expanded scale. The dashed line shows the path taken through these phase diagrams for a GaAs sample with $\hbar\Omega = 2$ meV as a function of B_\perp . (For GaAs $\tilde{\gamma} \sim 0.131(\hbar\Omega[\text{meV}])^2/(B_\perp[\text{T}])^{3/2}$ and $\tilde{g} \sim 0.0059B[\text{T}]/(B_\perp[\text{T}])^{1/2}$.) Regions of the phase diagram to the right of this line could be explored experimentally by using tilted magnetic fields.

Some qualitative features of these results can be understood rather simply by considering the competition between the Hartree and confinement energies. Assume that in the ground state electrons occupy the N_ϕ smallest- m orbitals with approximately equal probability, leading to a charge distribution which is approximately that of a uniform disk of radius [13] $R = \ell\sqrt{2N_\phi}$. (For such a state $M_z \sim NN_\phi/2$. The maximum value of N/N_ϕ allowed by the Pauli exclusion principle is 1 for spin-polarized states and 2 for unpolarized states.) For all but the smallest dots the two largest contributions to the total energy will be the Hartree and confinement energies,

$$E_H \sim \frac{8e^2N^2}{3\pi\epsilon R} = \frac{e^2}{\epsilon\ell} \frac{4\sqrt{2}}{3\pi} \frac{N^2}{N_\phi^{1/2}}, \quad (2)$$

$$E_C = \gamma(M_z + N) \sim \gamma NN_\phi/2. \quad (3)$$

Corrections due to exchange and correlations give a contribution proportional to N^1 for large N and are relatively less important for large dots. The confinement energy favors compact dots with small values of N_ϕ while the interaction energy favors expanded dots. For a given value of $\tilde{\gamma}$ and N the optimum dot size is determined by minimizing $E_H + E_C$ with respect to N_ϕ . This gives

$$\frac{N_\phi}{N} = \left(\frac{4\sqrt{2}}{3\pi\tilde{\gamma}N^{1/2}} \right)^{2/3}, \quad (4)$$

$$E_H + E_C = \frac{3}{2} [(e^2/\epsilon\ell)^2 \gamma (4\sqrt{2}/3\pi)^2]^{1/3} N^{5/3}, \quad (5)$$

and

$$\mu_N \sim \frac{5}{2} [(e^2/\epsilon\ell)^2 \gamma (4\sqrt{2}/3\pi)^2]^{1/3} N^{2/3}. \quad (6)$$

Note that in this approximation the energy and μ_N are independent of magnetic field. This result differs qualitatively from the constant interaction model where μ_N would be the sum of an interaction term proportional to N and a single-particle term. The difference is that here the size of the dot is not fixed but is determined by a competition of interaction and single-particle terms. Comparing with Figs. 1 and 2 we see that the values of the ground state angular momenta are reasonably estimated by Eq. (4) [$M_z \sim NN_\phi/2 \sim 0.36(N/\tilde{\gamma})^{2/3}$] even for $N = 5$ and $N = 6$. (Overestimates are expected since correlations will reduce the interaction energy cost of making the dots smaller.) In the Hartree-Fock generalization of the above argument, the exchange energy would stabilize the state with the largest spin polarization allowed by the Pauli exclusion principle for a given M_z . Indeed the most compact fully spin-polarized state [$M_z = N(N-1)/2$; $S_\alpha = N/2$], which is the precursor of the bulk $\nu = 1$ state, has a large range of stability in the phase diagrams of Figs. 1 and 2. However, many states with smaller values of S_α occur at larger M_z where full spin polarization is allowed. This is in direct contradiction with Hartree-Fock theory and is a result of correlations.

Figure 3 shows [14] the magnetic field dependence of μ_6 for a GaAs sample with $\hbar\Omega = 2$ meV. (The inset shows results for $N = 2, 3, 4, 5, 6$ on a wider energy scale.) The

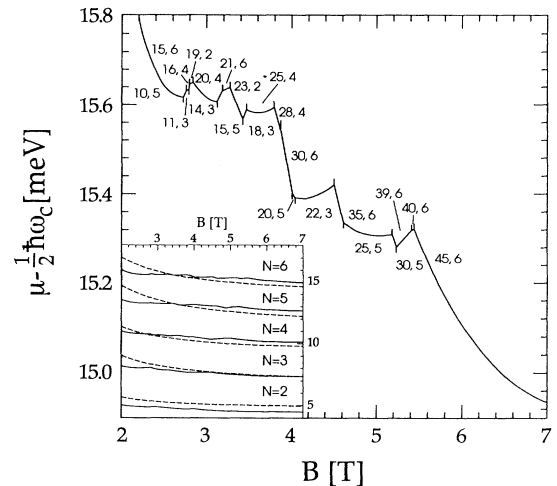


FIG. 3. Magnetic field dependence of the $N = 6$ addition spectrum for a parabolically confined quantum dot with $\hbar\Omega = 2$ meV. The curve has a cusp whenever there is a ground state level crossing for either the $N = 5$ or $N = 6$ dot. Curve segments between two upward tick marks are labeled with the ground state quantum numbers ($M_z, 2S_z$) of the $N = 6$ dot. Segments between downward tick marks are labeled with the quantum numbers of the $N = 5$ dot. The paths followed through the phase diagrams for this model are indicated by the dashed lines in Figs. 1 and 2. The inset shows results for $N = 2, 3, 4, 5, 6$ on a wider energy scale. The dashed lines are the best fit of the constant interaction model to our results.

sublinear increase in μ_N with N is consistent with the $N^{2/3}$ dependence predicted by Eq. (6). Similarly, the magnetic-field dependence is weaker than expected from the constant interaction model (dashed lines) and consistent with the approximate field independence predicted by Eq. (6). In approximate agreement with Eq. (4), the angular momentum difference between the $N = 5$ ground state and the $N = 6$ ground state increases from 5 to 15 in going from the left- to right-hand sides of the curve. However, the finer features apparent in the plot of μ_6 are a consequence of strong correlations and cannot be explained with Hartree-Fock or similar approximations. There are many cusps in μ_6 due to ground state level crossings of either $N = 5$ or $N = 6$ dots. At a ground state level crossing dE_0/dB must decrease. It follows that ground state level crossings in the $N - 1$ and N particle systems lead respectively to positive and negative cusps, as seen in Fig. 3. Note that unlike the prediction of an independent-particle approximation [2,3], upward and downward pointing cusps do not in general alternate. At the left-hand side ($B \sim 2.5$ T) of this figure both the $N = 5$ and $N = 6$ dots are in the $[M_z = N(N - 1)/2; S_\alpha = N/2]$ maximum-density spin-polarized states, while at the right-hand side ($B \sim 6$ T) both dots are in $[M_z = 3N(N - 1)/2; S_\alpha = N/2]$ states. These states are the precursors of the bulk $\nu = 1$ and $\nu = 1/3$ incompressible states and the incompressibility is reflected [9] in the relative large regions of stability in the phase diagrams. The resulting "plateaus" in the addition spectrum should be among the most visible features experimentally. Precursors of a filling-factor- ν state will occur for $N/N_\phi = \nu$; it follows from Eq. (4) that for GaAs we can expect associated features in the addition spectrum to occur for $B[\text{T}] \sim 0.363(\hbar\Omega[\text{meV}])^{4/3}N^{1/3}/\nu$. Features identified with $\nu = 2$ in the recent experiments of Ashoori *et al.* [3] seem to follow this $N^{1/3}$ law rather well. Unidentified experimental features which appear at approximately twice this field may be precursors of the $\nu = 1$ incompressible state. We predict that features associated with precursors of fractional incompressible states will appear at stronger fields and also, less visibly, at intermediate fields.

This work was supported by the National Science Foundation under Grant No. DMR-9113911 and by the UCF Division of Sponsored Research. A.H.M. acknowledges helpful conversations with Ray Ashoori, Mark Kastner, Horst Stormer, and Karen Tevosyan.

[1] For recent reviews, see U. Merkt, *Adv. Solid State Phys.* **30**, 77 (1990); Tapash Chakraborty, *Comments Condens. Matter Phys.* **16**, 35 (1992); M.A. Kastner, *Rev. Mod.*

Phys. **64**, 849 (1992).

- [2] P.L. McEuen, E.B. Foxman, U. Meirav, M.A. Kastner, Y. Meir, Ned S. Wingreen, and S.J. Wind, *Phys. Rev. Lett.* **66**, 1926 (1991); P.L. McEuen, E.B. Foxman, Jari Kinaret, U. Meirav, M.A. Kastner, Ned S. Wingreen, and S.J. Wind, *Phys. Rev. B* **45**, 11 419 (1992); E.B. Foxman, P.L. McEuen, U. Meirav, Ned S. Wingreen, Yigal Meir, Paul A. Belk, N.R. Belk, and M.A. Kastner, and S.J. Wind, *Phys. Rev. B* **47**, 10 020 (1993).
- [3] R.C. Ashoori, H.L. Stormer, J.S. Weiner, L.N. Pfeiffer, S.J. Pearton, K.W. Baldwin, and K.W. West, *Phys. Rev. Lett.* **68**, 3088 (1992); R.C. Ashoori, H.L. Stormer, J.S. Weiner, L.N. Pfeiffer, K.W. Baldwin, and K.W. West, *Phys. Rev. Lett.* **71**, 613 (1993).
- [4] Y. Meir, N.S. Wingreen, and P.A. Lee, *Phys. Rev. Lett.* **66**, 3048 (1991); C.W.J. Beenakker, *Phys. Rev. B* **44**, 1646 (1991).
- [5] Two-electron dots have been studied numerically by M. Wagner, U. Merkt, and A.V. Chaplik, *Phys. Rev. B* **45**, 1951 (1992), and by Daniela Pfannkuche, Vidar Gudmundsson, and Peter A. Maksym, *Phys. Rev. B* **47**, 2244 (1993).
- [6] P.A. Maksym and T. Chakraborty, *Phys. Rev. Lett.* **65**, 108 (1990); J.M. Kinaret, Yigal Meir, Ned S. Wingreen, Patrick Lee, and Xiao-Gang Wen, *Phys. Rev. B* **45**, 9489 (1992); N.F. Johnson and M.C. Payne, *Phys. Rev. Lett.* **67**, 1157 (1991).
- [7] For the small N quantum dots considered here the use of a parabolic confinement potential model is well justified. For quantum dots defined by gates the potential from external charges will change in a geometry-dependent way as the quantum dot is charged. These changes can often be accounted for in terms of phenomenological capacitances.
- [8] Calculations in the strong field limit typically require quantitative but not qualitative corrections when comparing with experiments performed at moderate magnetic fields.
- [9] Technical aspects of our calculations and comparisons with experiment will be discussed in more detail in a planned longer publication.
- [10] Sami Mitra and A.H. MacDonald, *Phys. Rev. B* **48**, 2005 (1993).
- [11] A.H. MacDonald and M.D. Johnson, *Phys. Rev. Lett.* **70**, 3107 (1993).
- [12] A.H. MacDonald, S.-R. Eric Yang, and M.D. Johnson, *Aust. J. Phys.* **46**, 345 (1993).
- [13] This is a good approximation for small dots whose ground state is related to an incompressible state of the 2D electron gas. For very large dots the classical semielliptical density profile will be approached; S. Nazin, K. Tevosyan, and V. Shikin, *Surf. Sci.* **263**, 351 (1992), and work cited therein.
- [14] A code which generates addition spectra from the many-electron eigenenergy data sets is available from the authors for use in interpreting experimental results.